Stem Cell Reports, Volume *17*

Supplemental Information

Characterization of N-terminal RYR2 variants outside CPVT1 hotspot regions using patient iPSCs reveal pathogenesis and therapeutic potential

Marissa J. Stutzman, C.S. John Kim, David J. Tester, Samantha K. Hamrick, Steven M. Dotzler, John R. Giudicessi, Marco C. Miotto, Jeevan B. GC, Joachim Frank, Andrew R. Marks, and Michael J. Ackerman

Supplemental Figures

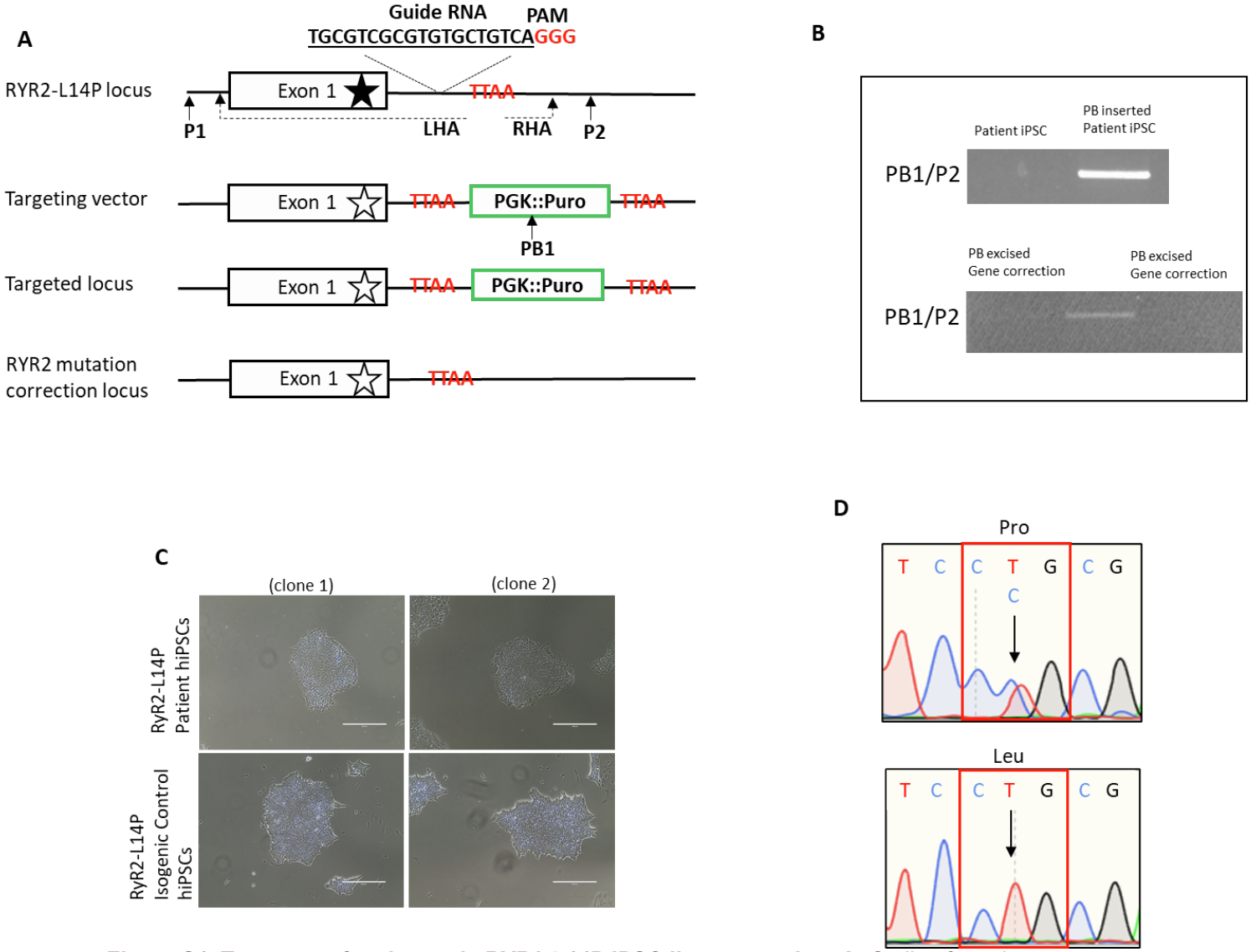

Figure S1. Transgene-free isogenic RYR2-L14P iPSC line generation. A. Outline for using CRISPR/Cas9 and PiggyBac system to generate transgene-free isogenic control cell line. Black and white stars denote p.14P and p.14L, respectively. Green box represents PiggyBac backbone. **B.** Selection of gene corrected clones from agarose gel images. Successful insertion of PiggyBac vector produces a band shown in top panel. Bottom panel shows no bands, indicating removal of PiggyBac cassette. **C.** Phase-contrast light images from RYR2-L14P and isogenic control iPSC colonies. Scales bars represent 400µm. **D.** Sanger sequencing chromatograms showing RYR2-L14P variant in patient iPSCs and variant correction in isogenic control iPSCs.

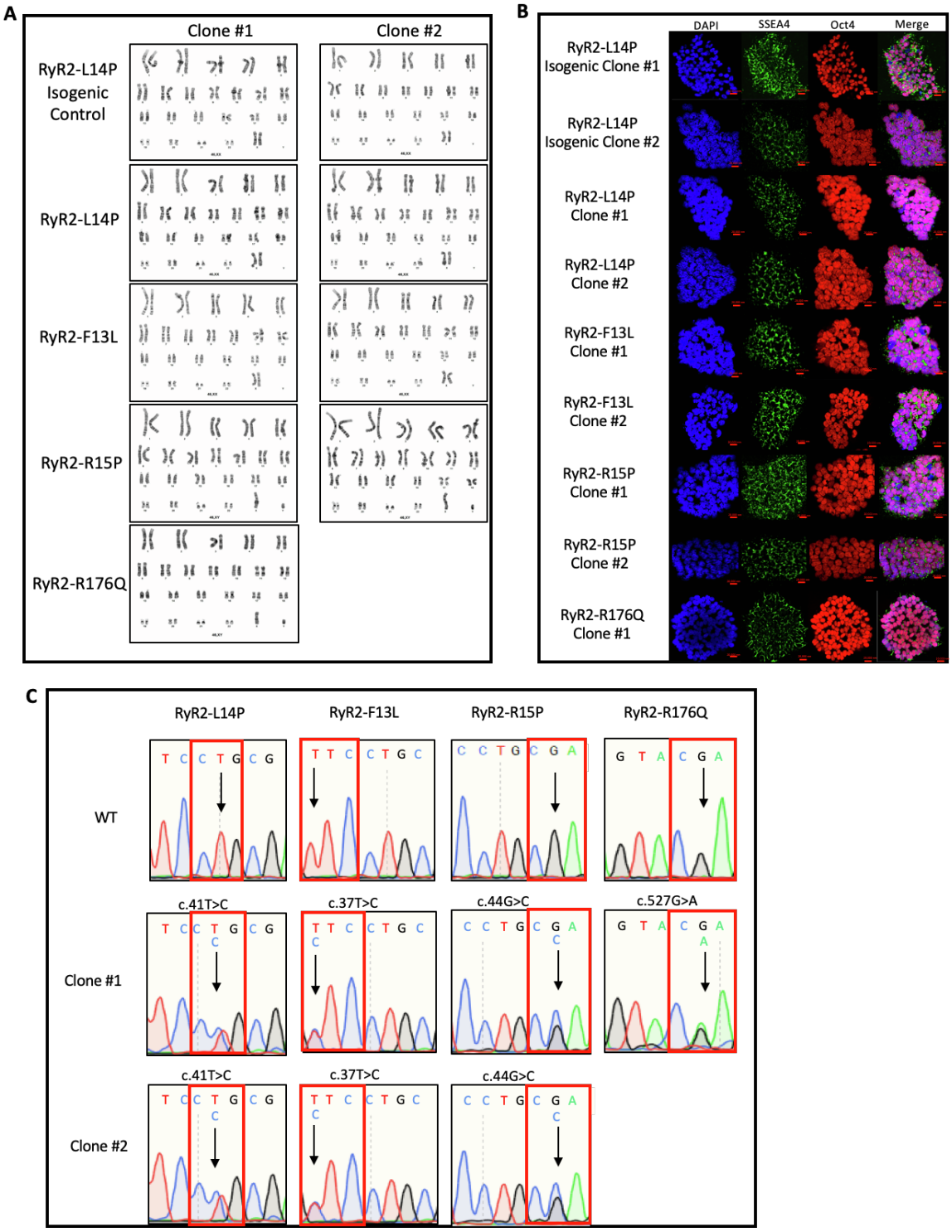

Figure S2. A. All clones of N-term, RYR2-L14P isogenic control, and classical CPVT iPSCs displayed normal karyotypes. **B**. Each clone for N-term, isogenic control, and classical CPVT iPSCs demonstrated expression of SSEA4 and Oct4 pluripotency markers. Scale bars equal 20,000 nm. **C.** Sanger sequencing chromatograms confirmed *RYR2* variants in iPSCs derived from patients. Wild-type sequencing provided for comparison. Arrows denote heterozygous variant present in iPSCs.

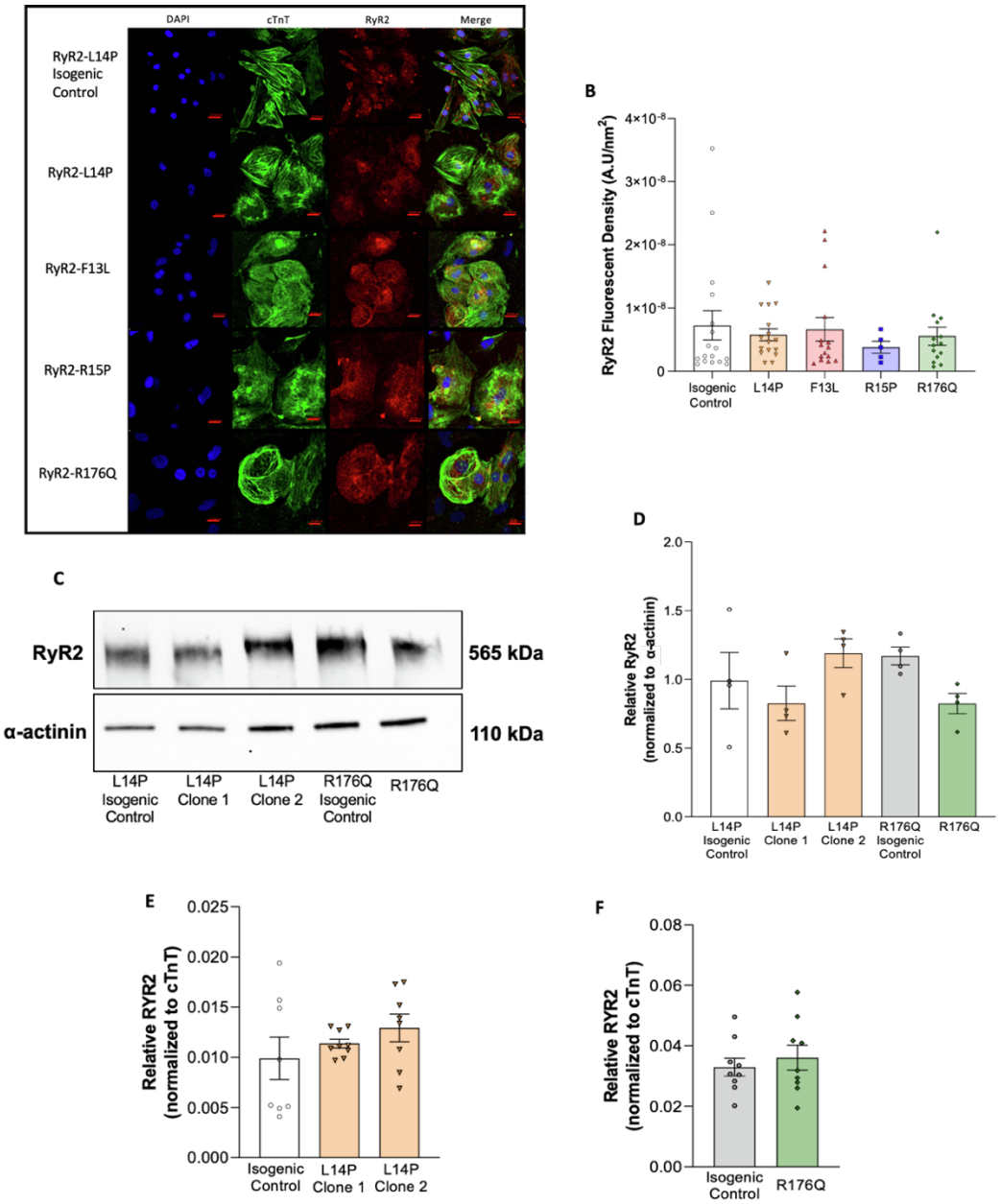

Figure S3. A. Representative immunofluorescence (IF) images of RYR2 and Cardiac Troponin (cTnT) merged with DAPI staining for isogenic control, N-term, and classical CPVT (RYR2-R176Q) iPSC-CMs. Scale bars equal 20,000 nm. **B.** Quantification of RYR2 protein expression in isogenic control, N-term, and classical CPVT iPSC-CMs. Data presented as mean ± SEM. A one-way ANOVA was performed with post-hoc Tukey-Kramer testing. **C.** Western blot detecting RYR2 and α-actinin in L14P isogenic control (lane 1), L14P clone 1 (lane 2), L14P clone 2 (lane 3), R176Q isogenic control (lane 4), and R176Q (lane5) iPSC-CMs. **D.** ImageJ quantification of Western blot pixel density of RYR2 normalized to α-actinin. Data presented as mean ± SEM. A one-way ANOVA and Tukey-Kramer post-hoc test was performed for comparisons. **E.** Relative *RYR2* expression for L14P isogenic control and L14P variant iPSC-CM clones normalized to *cTnT* measured by qRT-PCR. Data presented as mean ± SEM. A one-way ANOVA and Tukey-Kramer post-hoc test was performed for comparisons. **F.** Relative *RYR2* expression for R176Q isogenic control and R176Q variant iPSC-CMs normalized to *cTnT* measured by qRT-PCR. Data presented as mean ± SEM. 3 independent experiments were conducted. A student's t-test was performed to determine statistical significance between two groups. iPSC-CMs used were 30-50 days old.

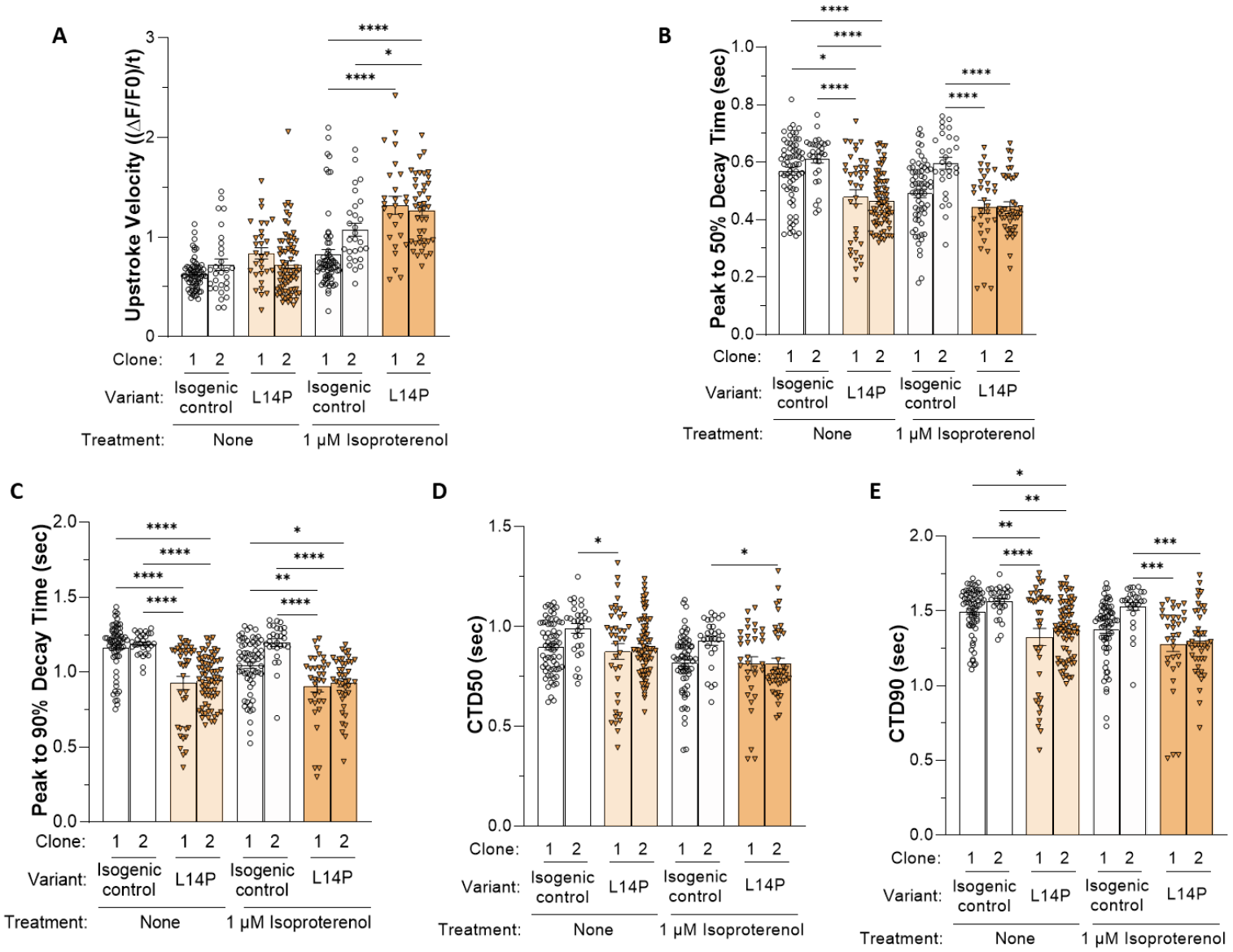

Figure S4. Altered calcium handling kinetics in RYR2-L14P iPSC-CMs. A. Calcium transient upstroke velocity, **B.** Calcium transient decay 50%, **C.** Peak to 90% decay time, **D.** Calcium transient duration 50%, and **E.** 90% of isogenic control and L14P iPSC-CMs at baseline and following treatment with 1μM ISO measured by Fluo-4 calcium imaging. Data presented as mean ± SEM. n = 26-71 per group (Table S1). 3-8 independent experiments were conducted. A two-way ANOVA was performed with post-hoc Tukey-Kramer testing. *p<0.05, **p<0.01, ***p<0.001, ****p<0.0001. iPSC-CMs used were 30-50 days old. See also Figure 2.

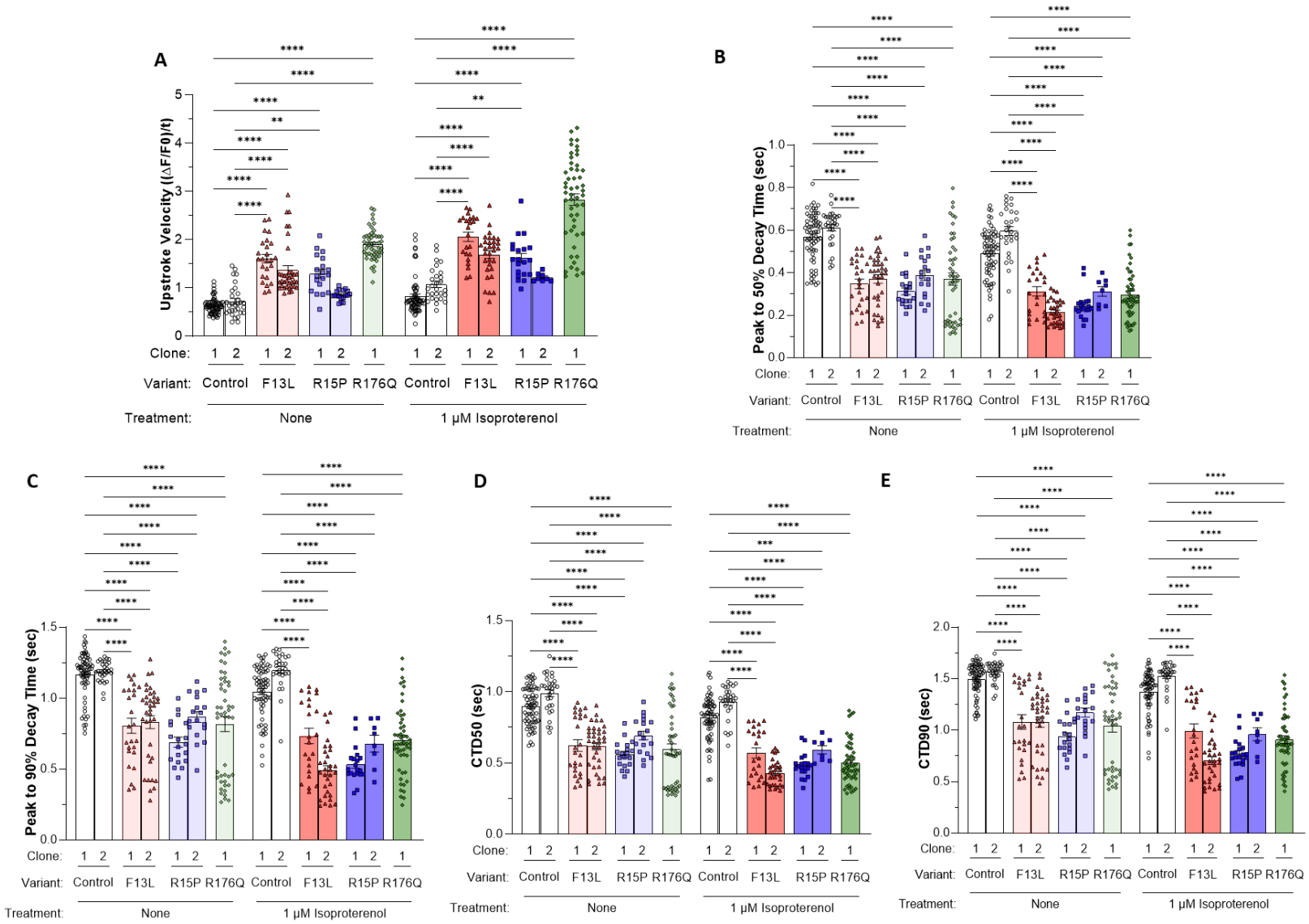

Figure S5. Calcium handling kinetics in RYR2-F13L, -R15P, and -R176Q iPSC-CMs. A. Calcium transient upstroke velocity, **B.** Calcium transient decay 50%, **C.** Peak to 90% decay time, **D.** Calcium transient duration 50%, and **E.** Calcium transient duration 90% of control, -F13L, -R15P, and -R176Q iPSC-CMs at baseline and following treatment with 1μM ISO measured by Fluo-4 calcium imaging. Data presented as mean ± SEM. n = 8-67 per group (Table S1). 3-7 independent experiments were conducted. A two-way ANOVA was performed with post-hoc Tukey-Kramer testing. *p<0.05, **p<0.01, ***p<0.001, ****p<0.0001. iPSC-CMs used were 30-50 days old. See also Figure 3.

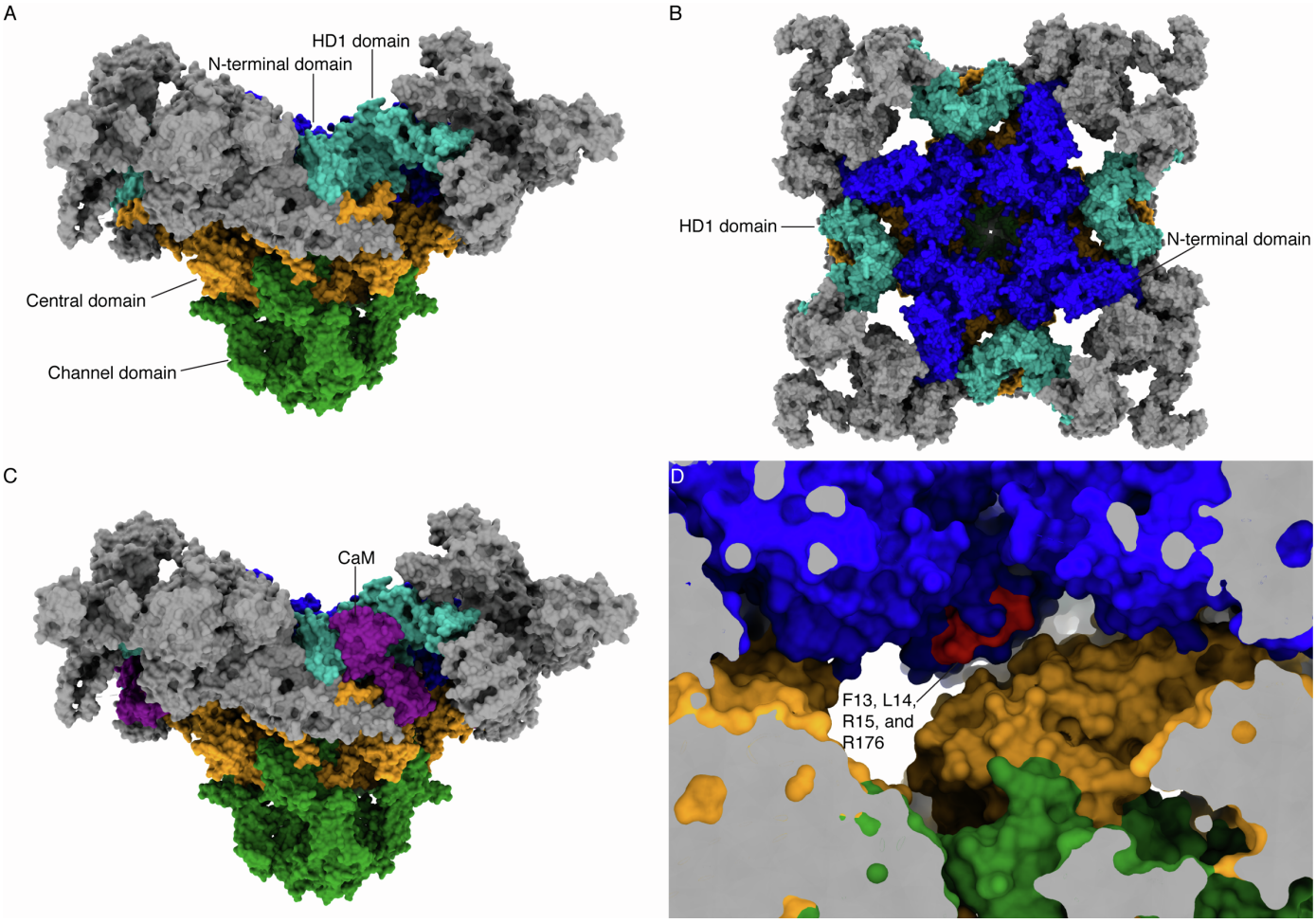

Figure S6. A-B. Representation of the atomic model of RYR2 (pdb: 6JI8) from the side (A) and top (B) views. The N-terminal domain (blue), HD1 domain (cyan), Central domain (orange), and Channel domain (green) are colored to differentiate from the other domains. **C.** Same as A, but CaM is included (purple) to show interaction with the HD1 and Central domains. **D.** View from the inside of the model showing the proximity of the N-terminal domain residues analyzed in this study (red) with the Central domain. Visualization and images were obtained with ChimeraX software (Pettersen et al. Protein Sci. 2021 Jan;30(1):70-82).

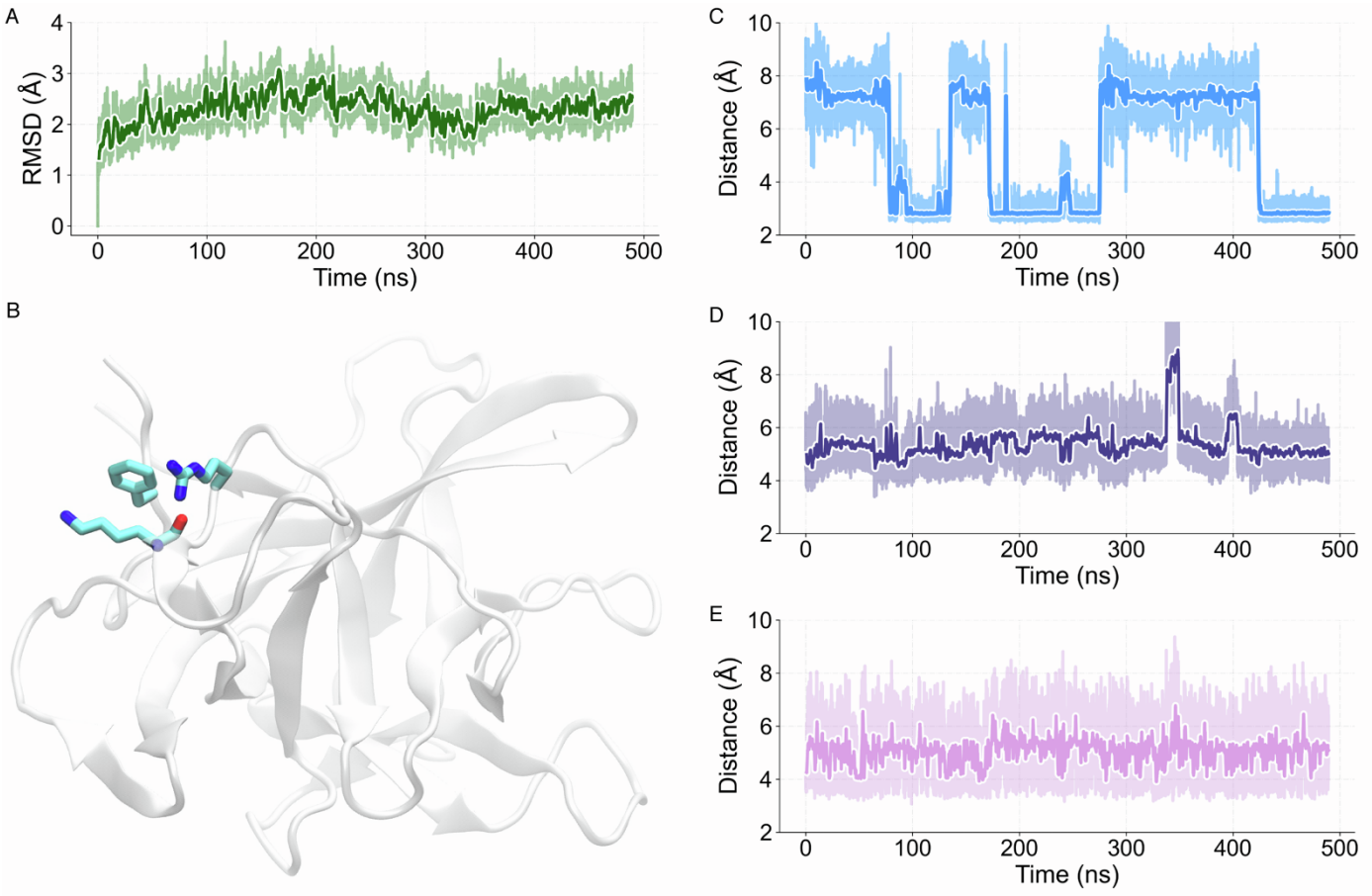

Figure S7. A. RMSD of the backbone atoms of RYR2 N-terminal domain, showing that the system remained stable during the simulation. RMSD is calculated using the backbone residues, and the values plateaued and remained below 3Å. **B.** Representative frame of the MD simulation showing the position of residues F13, R176 and K174. **C-E.** Plot showing the distance between R176 side-chain N-atom and K174 backbone O-atom (C), the center of mass of F13 sidechain and R176 CG-atom (D), and the center of mass of F13 sidechain and K174 CE-atom (E).

SUPPLEMENTAL TABLES

Table S1. Calcium handling properties from isogenic control, N-term, and classical CPVT iPSC-CMs at baseline (BL) and following 1μM isoproterenol (ISO).

iPSC	BL Amplitude	BL Upstroke Velocity	BL 50% Decay time	BL 90% Decay time	BL Calcium Transient Duration 50%	BL Calcium Transient Duration 90%	BL Ca^{2+} Sparks	ISO Amplitude	ISO Upstroke Velocity	ISO 50% Decay time	ISO 90% Decay time	ISO Calcium Transient Duration 50%	ISO Calcium Transient Duration 90%	ISO Ca^{2+} Sparks
Isogenic control #1	0.32±0.01 n=67	0.63± 0.02 n=67	0.57± 0.01 n=67	1.2± 0.02 n=67	0.90±0.02 n=67	1.5±0.02 n=67	0%±0 n=11	0.40±0.02 n=65	0.83±0.05 n=65	0.49± 0.01 n=65	1.0± 0.02 n=65	0.81± 0.02 n=65	1.4±0.03 n=65	0%±0 n=34
Isogenic control #2	0.38±0.02 n=30	0.72± 0.06 n=30	0.61± 0.02 n=30	1.2± 0.01 n=30	0.99±0.02 n=30	1.6±0.02 n=30	0%±0 n=6	0.51±0.02 n=28	1.1±0.07 n=28	0.60± 0.02 n=28	1.2± 0.03 n=28	0.93± 0.02 n=28	1.5±0.03 n=28	0%±0 n=22
RYR2-L14P clone #1	0.50±0.03 n=30	0.83± 0.06 n=30	0.48± 0.03 n=38	0.93± 0.04 n=38	0.88±0.04 n=38	1.3±0.06 n=38	46%± 15 n=5	0.73±0.03 n=26	1.3±0.09 n=26	0.44± 0.02 n=33	0.91± 0.04 n=33	0.81± 0.03 n=33	1.3±0.05 n=33	49%±5 n=27
RYR2-L14P clone #2	0.49±0.02 n=72	0.72± 0.04 n=72	0.47± 0.01 n=71	0.95± 0.02 n=71	0.90±0.02 n=71	1.4±0.02 n=71	25%±6 n=14	0.68±0.03 n=42	1.3±0.05 n=42	0.45± 0.02 n=42	0.93± 0.03 n=42	0.81± 0.03 n=42	1.3±0.03 n=42	42%±3 n=53
RYR2-F13L clone #1	0.60±0.04 n=25	1.6±0.09 n=25	0.35± 0.02 n=25	0.81± 0.05 n=25	0.62± 0.04 n=25	1.1± 0.07 n=25	21%±7 n=5	0.76±0.04 n=23	2.1±0.1 n=23	0.31± 0.02 n=23	0.73± 0.05 n=23	0.57± 0.04 n=23	0.99± 0.07 n=23	63%±4 n=19
RYR2-F13L clone #2	0.47±0.02 n=36	1.4±0.09 n=36	0.37± 0.02 n=36	0.83± 0.05 n=36	0.62± 0.03 n=36	1.1± 0.05 n=36	38%± 10 n=11	0.57±0.02 n=31	1.7±0.08 n=31	0.22± 0.01 n=31	0.49± 0.03 n=31	0.43± 0.02 n=31	0.71± 0.04 n=31	68%±5 n=19
RYR2-R15P clone #1	0.47±0.03 n=19	1.3±0.09 n=19	0.31± 0.02 n=19	0.69± 0.04 n=19	0.56± 0.02 n=19	0.94± 0.04 n=19	57%± 15 n=5	0.58±0.03 n=20	1.6±0.1 n=20	0.24± 0.01 n=20	0.53± 0.03 n=20	0.48± 0.02 n=20	0.77± 0.03 n=20	54%±7 n=11
RYR2-R15P clone #2	0.40±0.01 n=18	0.90± 0.02 n=18	0.39± 0.02 n=18	0.87± 0.04 n=18	0.69± 0.03 n=18	1.2± 0.04 n=18	44%± 29 n=2	0.52±0.02 n=8	1.2±0.03 n=8	0.31± 0.02 n=8	0.68± 0.06 n=8	0.59± 0.03 n=8	0.96± 0.06 n=8	62%±3 n=10
RYR2-R176Q clone #1	0.63±0.03 n=48	1.9±0.05 n=48	0.37± 0.03 n=48	0.82± 0.05 n=48	0.60± 0.04 n=48	1.0± 0.06 n=48	26%±8 n=10	0.84±0.03 n=52	2.8±0.1 n=52	0.30± 0.02 n=52	0.70± 0.03 n=52	0.50± 0.02 n=52	0.91± 0.04 n=52	47%±5 n=22

Data presented as mean ± SEM. A two-way ANOVA was performed with post-hoc Tukey-Kramer testing.

Table S2. Calcium handling properties from isogenic control and RYR2-L14P iPSC-CMs with and without nadolol (Nad), flecainide (Flec), and combination treatment at BL and following 1μM ISO.

iPSC	BL Amplitude	BL Ca^{2+} Sparks	ISO Amplitude	ISO Ca^{2+} Sparks
Isogenic Control	0.34±0.01 n=97	0%±0 n=17	0.44±0.02 n=93	0%±0 n=56
RYR2-L14P	0.47±0.01 n=92	31%±6 n=19	0.70±0.02 n=68	44%±3 n=80
RYR2-L14P + Nadolol	0.36±0.01 n=35	11%±3 n=11	0.45±0.02 n=30	11%±2 n=34
RYR2-L14P + 10μM Flecainide	0.44±0.03 n=15	5%±4 n=12	0.70±0.03 n=15	13%±3 n=20
RYR2-L14P + 25μM Flecainide	0.38±0.02 n=10	2%±2 n=4	0.49±0.04 n=10	15%±4 n=9
RYR2-L14P + Nadolol + Flecainide	0.38±0.03 n=9	4%±4 n=3	0.44±0.02 n=10	15%±2 n=6

Data presented as mean ± SEM. A one-way ANOVA was performed with post-hoc Tukey-Kramer testing.

Table S3. Calcium handling properties from control, RYR2-F13L, -R15P, and -R176Q iPSC-CMs with and without Nadolol treatment at BL and following 1μM ISO.

iPSC	BL Amplitude	BL Ca^{2+} Sparks	ISO Amplitude	ISO Ca^{2+} Sparks
Control	0.34±0.01 n=97	0%±0 n=17	0.44±0.02 n=93	0%±0 n=56
RYR2-F13L	0.52±0.02 n=61	33%±7 n=16	0.65±0.03 n=54	65%±3 n=38
RYR2-F13L + Nadolol	0.33±0.02 n=36	3%±2 n=14	0.45±0.02 n=39	20%±3 n=36
RYR2-R15P	0.44±0.02 n=37	53%±12 n=7	0.56±0.02 n=28	58%±4 n=21
RYR2-R15P + Nadolol	0.36±0.02 n=21	0%±0 n=6	0.41±0.01 n=22	5%±2 n=20
RYR2-R176Q	0.63±0.03 n=48	26%±8 n=10	0.84±0.03 n=52	47%±5 n=22
RYR2-R176Q + Nadolol	0.44±0.01 n=20	1%±1 n=5	0.63±0.03 n=20	5%±2 n=10

Data presented as mean ± SEM. A one-way ANOVA was performed with post-hoc Tukey-Kramer testing.

Video S1. Isogenic control + 1μM ISO Fluo-4 calcium imaging. Time lapse video recorded at 20ms per frame for 20s at 10% LED power. Isogenic control iPSC-CMs were treated with Fluo-4 calcium dye and paced at 0.5Hz.

Video S2. RYR2-L14P Variant + 1μM ISO Fluo-4 calcium imaging. Time lapse video recorded at 20ms per frame for 20s at 10% LED power. RYR2-L14P iPSC-CMs were treated with Fluo-4 calcium dye and paced at 0.5Hz.

Video S3. RYR2-R176Q Variant + 1μM ISO Fluo-4 calcium imaging. Time lapse video recorded at 20ms per frame for 20s at 10% LED power. RYR2-R176Q iPSC-CMs were treated with Fluo-4 calcium dye and paced at 0.5Hz.

Video S4. Molecular dynamic simulation (MDS). MDS of the N-terminal domain, focused on the residues of interest F13, K174 and R176.

SUPPLEMENTAL EXPERIMENTAL PROCEDURES

Generation of Patient-Specific iPSCs

Dermal samples were collected from 4 mm punch biopsies. Peripheral blood mononuclear cells and fibroblasts were reprogrammed by Sendai virus transduction using the Cytotune 2.0 Sendai Reprogramming Kit (Thermofisher: A16517). Within 21 days after infection, colonies were picked and clonally expanded according to ReGen Theranostics protocols.

Mutation Correction of RYR2-L14P using CRISPR/Cas9

Cloning of the left and right homologous arms into the MV-PGK-Puro-TK PiggyBac vector was achieved using enzyme restriction sites BsiW1 and Not1 for the right arm, and ASC1 and Nsi1 for the left arm. The homologous arms were separately digested, gel purified, and finally ligated into the vector.

To avoid choosing clones containing random integration, primers P1 and P2 were designed outside of the homology arms to detect homologous recombination, while PB1 was designed inside of the PiggyBac cassette. DNA was extracted from the 712-bp band and used for Sanger sequencing. All primers are listed as follows; Guidance RNA, 5'-TGCGTCGCGTGTGCTGTCA-3'; P1 (outside of LHA), 5'-CCCGATTCCCAGCGCAGCCAGTA-3'; P2 (outside of RHA), 5'- GGTCACAGCACCACCACGGATG-3'; PB1 (inside of PiggyBac Cassette), 5'- CGTCAATTTTACGCATGATTATCTTTAAC-3'.

Differentiation into iPSC-CMs

iPSCs were cultured on Matrigel coated 6-well plates in mTeSR1 media and incubated at 37°C and 5% CO_2. At 85% confluency, iPSCs were disaggregated with ReLeSR™ (STEMCELL Tech., 05872), passaged into 24-well plates, and grown for 2-4 days to create a monolayer. The differentiation strategy used has been previously reported (Mummery et al. 2012, Burridge et al. 2014). At 90% confluency, the culture medium was changed to RPMI 1640 supplemented with B27-minus Insulin (Gibco, A18956-01) containing CHIR99021 (TOCRIS, 4423, 5μM as working concentration) for 48 hours. On day 2, RPMI-B27-minus insulin medium containing IWP2 (TOCRIS, 3533, 5μM as working concentration) was added for 48 hours. On day 4, RPMI-B27-minus insulin medium was added, and cells were maintained in this medium for 10-12 days until beating appeared. At 10-12 days post differentiation, the medium was changed to RPMI 1640 basal medium supplemented with 500 μg/ml of recombinant human albumin (Sigma, A9731), 217 μg/ml of L-ascorbic acid 2-phosphate (Sigma, A8960) and 5 mM of DL-Lactate (Sigma, L4263) to select for cardiomyocytes reported (Mummery et al. 2012, Burridge et al. 2014, Fuerstenau-Sharp et al. 2015). After 7 days of selection, the cardiomyocytes were maintained in RPMI supplemented with B27 Plus Supplement (Gibco, A3582801) and 1%Pen/Strep.

Dissociation of iPSC-CMs

At 30-50 days, iPSC-CMs were washed once with PBS (without Ca/Mg) and then enzymatically dissociated using STEMdiff™ cardiomyocyte dissociation kit (STEMCELL Technologies, 05025) for 30 seconds to 1 minute (Froese et al. 2018). Dissociation solution was removed and cells were incubated for 3-6 minutes. Dissociation was deactivated by the addition of cardiomyocyte support media. Cells were then triturated and plated into the appropriate dishes for subsequent assays. The following day, the medium was changed back to RPMI-B27 plus supplement.

Western Blot for RYR2

iPSC-CMs were lysed in RIPA buffer (EMD Millopore, Burlington, MA) with Protease Inhibitor Cocktail (TaKaRa, Mountain View, CA). Lysates were mixed 1:1 with 2X Laemmli buffer + 2-Mercaptoethanol, denatured at 95°C for 5 min, and loaded on a 4-15% TGX gel (Bio-Rad, Hercules, CA). Protein was transferred onto a PVDF membrane using a Trans-Blot Turbo Transfer System (Bio-Rad, Hercules, CA). The membrane was blocked for 1 hour in tris-buffered saline (TBS) with 0.1% Tween-20/3% bovine serum albumin and then incubated with primary antibodies against RYR2 (1:1,000 dilution, mouse, ThermoFisher, MA3-916) or α-Actinin (1:1,000 dilution, mouse, Sigma, A7811) overnight at 4°C. Membranes were then incubated in secondary antibody (Goat anti-rabbit, 1:10,000, Invitrogen, Carlsbad, CA, 656120; Goat anti-mouse, 1:10,000 R&D Systems, Minneapolis, MN, HAF007) for 1 hour at RT. Finally, the membrane was incubated with either SuperSignal West Pico PLUS chemiluminescent ECL substrate (ThermoFisher, Waltham, MA) for 5 min or SuperSignal West Femto Maximum Sensitivity chemiluminescent ECL substrate for 5 min and imaged using the iBright CL1500 Imaging System (ThermoFisher, Waltham, MA). Pixel density of all quantified proteins was measured using freely available ImageJ software and normalized to α-Actinin. There was no change in *RYR2* protein expression between isogenic control and *RYR2* missense variant-containing iPSC-CMs (**Figure S3C-D**).

qRT-PCR of iPSC-CMs

iPSC-CMs were collected at 30-40 days post differentiation. RNA was harvested using the RNeasy kit [Qiagen] and measured using the NanoDrop ND-1000 spectrophotometer [Thermo]. *RYR2* and *cTnT* primers were purchased from IDT [Coralville, IA]. The cDNA was prepared from 60 ng of RNA using the QuantiTect Reverse Transcription Kit (Qiagen, 205311) according to the manufacturer's instruction. Gene expression levels for *RYR2* and a cardiac-specific control (*cTnT*) gene was performed using the 7900 Real-time (RT) polymerase chain reaction (PCR) system (Applied Biosystems). Relative gene expression analysis was performed using a modified $\Delta\Delta$Ct method employing the Pfaffl formula which accounts for PCR amplification efficiencies between primer sets. Statistical analysis was performed using GraphPad Prism (GraphPad Software). Three biological replicates were used for each iPSC-CM line. There was no change in *RYR2* gene expression between isogenic control and *RYR2* missense variant-containing iPSC-CMs (**Figure S3E-F**).

Primer sequences used in RT-qPCR

Name	Sequence (5' to 3')
RYR2-Forward	GGAGTCCACTTCCAATTCCA
RYR2-Reverse	CTCTTGCAAGCCAACATCAA
cTnT-Forward	TTCACCAAAGATCTGCTCCTCGCT
cTnT-Reverse	TTATTACTGGTGTGGAGTGGGTGTGG

Immunocytochemistry of iPSCs and iPSC-CMs

iPSCs or 30-day old iPSC-CMs were harvested and using the STEMCELL Technologies protocol previously described and plated into 8-chamber slides. Cells were grown for 2-4 days, then washed once with PBS and subjected to fixation with 4% paraformaldehyde for 10 minutes at room temperature (RT) followed by being washed 3 times with PBS. The iPSCs or iPSC-CMs were blocked with 0.1% Triton X-100/ PBS (PBST)/5% goat serum for 1 hour at RT, then incubated at 4 ^{o}C overnight in primary antibody solution consisting of PBST/5% goat serum containing a 1:250 dilution of Oct4 (ThermoFisher, PA5-27438) and SSEA-4 (ThermoFisher, MA1-021) for iPSCs, or cTnT (Abcam, ab45932) and RYR2 (ThermoFisher, MA3-916) for iPSC-CMs. The following day, cells were washed 3 times with PBST/5% goat serum at RT before being incubated for 1 hour in PBST/5% goat serum with Alexa Fluor® 488 goat-anti-rabbit (ThermoFisher, A-11008) and Alexa Fluor® 594 goat-anti-mouse (ThermoFisher, A-11005) secondary antibodies at a dilution of 1:200µL. After secondary antibody incubation, cells were washed 3 times with PBST and DAPI was added to the final wash at dilution of 1:2000 µL. Mounting solution and coverslips were added to slides. Images were acquired on a Zeiss LSM 780 confocal microscope in the Mayo Microscopy and Flow Cytometry Cell Analysis Core Facility. Zen Blue (ZEISS, Germany) analysis software was used to quantify fluorescence.

Conformational Dynamics of RYR2 N-Terminal Domain Using Molecular Dynamics (MD) Simulations

RYR2 N-terminal domain structure preparation

The N-terminal domain was loaded into Maestro and processed using Schrödinger's Protein Preparation Wizard Panel (Sastry et al. 2013) with default options such as missing hydrogen atoms and sidechain atoms and optimization of hydrogen bonding networks. Also, the optimal protonation states for histidine residues capped the N- and C- terminal ends with acetyl (ACE) and methyl amide (NMA) groups, respectively. Finally, the preprocessed structure was restraint minimized using an OPLS forcefield that minimizes hydrogen atoms while restraining the backbone and sidechain heavy atoms. The final structure was further solvated in the cubic box with explicit water and ions for further MD simulations.

Molecular Dynamics (MD) Simulations

The N-terminal domain was solvated in a cubic box with a dimension of 67.0 x 67.0 x 67.0 Å^3. The system contained 0.15 M NaCl, and simulations were conducted at 310 K. The interaction between protein, water residues are modeled using CHARMM36 force field(Klauda et al. 2010) and TIP3P water.(Jorgensen et al. 1983) All simulations were run using GROMACS v5.1.4.(Mark James Abraham 2015) The MD simulation protocol starts with energy minimization of 1000 steps, followed by constant atoms, volume, and temperature (NVT) equilibration (1 fs per time step) and NPT (2 fs per time step) simulations for five ns prior to starting the production simulations. During the initial minimization and equilibration, the backbone, sidechain, and dihedral restraint were applied, and in the production, the run protein was allowed to move

freely without any restraint. Temperature and pressure during the equilibration phase were maintained at 310 K and 1 bar, respectively, using Berendsen thermostat and barostat.(Berendsen et al. 1984) For the production run, a Nose-Hoover thermostat was used to control the temperature using a collision frequency of 1.0 ps^{-1}. Lennard-Jones and electrostatic interactions were calculated explicitly within a cutoff of 1.2 nm, and long-range electrostatic interactions were calculated by particle mesh Ewald summation. The equilibration simulations are done on the NVT ensemble, and production run at constant atoms, pressure, and temperature (NPT) ensemble for 500ns.

Analysis

All unique H-bonds in N-terminal domain residues were calculated using a cutoff distance of 3.5 Å and a cutoff angle of 45° between acceptor and donor atoms. Bond occupancies were gathered by taking the sum of individual occurrences over the full trajectory. Root mean square deviation (RMSD) was calculated using the RMSD trajectory tool in VMD. The distance between the center of mass (COM) of atoms was calculated using the VMD in-house tcl scripts. All other time series figures are generated using Python scripts.

References

Berendsen, H. J. C., J. P. M. Postma, W. F. Vangunsteren, A. Dinola and J. R. Haak (1984). "Molecular-Dynamics with Coupling to an External Bath." Journal of Chemical Physics **81**(8): 3684-3690.

Burridge, P. W., E. Matsa, P. Shukla, Z. C. Lin, J. M. Churko, A. D. Ebert, F. Lan, S. Diecke, B. Huber, N. M. Mordwinkin, et al. (2014). "Chemically defined generation of human cardiomyocytes." Nat Methods **11**(8): 855-860.

Froese, N., H. Wang, C. Zwadlo, Y. Wang, A. Grund, A. Gigina, M. Hofmann, K. Kilian, G. Scharf, M. Korf-Klingebiel, et al. (2018). "Anti-androgenic therapy with finasteride improves cardiac function, attenuates remodeling and reverts pathologic gene-expression after myocardial infarction in mice." Journal of Molecular and Cellular Cardiology **122**: 114-124.

Fuerstenau-Sharp, M., M. E. Zimmermann, K. Stark, N. Jentsch, M. Klingenstein, M. Drzymalski, S. Wagner, L. S. Maier, U. Hehr, A. Baessler, et al. (2015). "Generation of highly purified human cardiomyocytes from peripheral blood mononuclear cell-derived induced pluripotent stem cells." PloS one **10**(5): e0126596-e0126596.

Jorgensen, W. L., J. Chandrasekhar, J. D. Madura, R. W. Impey and M. L. Klein (1983). "Comparison of Simple Potential Functions for Simulating Liquid Water." Journal of Chemical Physics **79**(2): 926-935.

Klauda, J. B., R. M. Venable, J. A. Freites, J. W. O'Connor, D. J. Tobias, C. Mondragon-Ramirez, I. Vorobyov, A. D. MacKerell, Jr. and R. W. Pastor (2010). "Update of the CHARMM all-atom additive force field for lipids: validation on six lipid types." J Phys Chem B **114**(23): 7830-7843.

Mark James Abraham, T. M., Roland Schulz, Szilárd Páll, Jeremy C. Smith, Berk Hess, Erik Lindahl (2015). "GROMACS: High performance molecular simulations through multi-level parallelism from laptops to supercomputers." SoftwareX **1-2**: 19-25.

Mummery, C. L., J. Zhang, E. S. Ng, D. A. Elliott, A. G. Elefanty and T. J. Kamp (2012). "Differentiation of human embryonic stem cells and induced pluripotent stem cells to cardiomyocytes: a methods overview." Circ Res **111**(3): 344-358.

Sastry, G. M., M. Adzhigirey, T. Day, R. Annabhimoju and W. Sherman (2013). "Protein and ligand preparation: parameters, protocols, and influence on virtual screening enrichments." J Comput Aided Mol Des **27**(3): 221-234.